Available online at www.sciencedirect.com
SCIENCE DIRECT®
Biochemical and Biophysical Research Communications 312 (2003) 255–261
BBRC
www.elsevier.com/locate/ybbrc

g-Strain, ENDOR, and structure of active centers of two-iron ferredoxins

W. Richard Dunham[a,*] and Richard H. Sands[b]

[a] *Department of Surgery, The University of Michigan Health System, Ann Arbor, MI 48109-0592, USA*
[b] *Department of Physics, University of Michigan, Ann Arbor, MI 48109-1020, USA*

Received 25 September 2003

Abstract

Collaborative chemical and spectroscopic work from several laboratories resulted in a qualitative structure for the active center in the two-iron ferredoxins, with each iron being in a distorted tetrahedron of sulfur atoms (two acid-labile sulfurs bridging the two iron atoms and the other two from cysteine sulfurs). Subsequent X-ray data from other laboratories confirmed this structure. Detailed EPR spectral syntheses showed that there is a distribution of structures in any given protein (even in a single crystal) resulting in a distribution of the principal values of the *g* tensor, which may be described by a statistical distribution of still another tensor whose principal axes are, in general, not coincident with the principal-axis frame of the *g* tensor.
© 2003 Elsevier Inc. All rights reserved.

We first interacted with Professor I.C. Gunsalus (Gunny) in the 1960s when several scientists from a variety of disciplines were working collaboratively at several institutions to discover the nature of the active site in the two-iron ferredoxins. At the time, Gunny and a research associate of his, J.C.M. Tsibris, in the Department of Biochemistry, University of Illinois, were studying the two-iron ferredoxin from the bacterium *Pseudomonas putida*. Because no one currently was able to grow large single crystals of these proteins, it was necessary to apply a variety of chemical and spectroscopic techniques in an effort to delineate the nature and structure of the active sites in these proteins. Gunny and Tsibris generously provided samples of their protein for EPR and ENDOR studies by our students and us. Gunny and Dr. Helmut Beinert from the Enzyme Institute at the University of Wisconsin were the senior members of these collaborations, and they provided much appreciated maturity and leadership. The resulting collaborations were enjoyed by all. [One of us (R.H.S.) shared a love for fine wines with Gunny. It was Gunny's practice to travel through the Burgundy district of France every spring, to sample wines and order specific wines to be shipped to his home in Champaign-Urbana. He had no source for German whites; however, R.H.S. belonged to a wine club in Ann Arbor and was able to procure several fine German wines. Needless to say, several trades were arranged over the years to the mutual enjoyment of Gunny and Sands and their friends.]

Two-iron ferredoxins, low-molecular-weight proteins of unusually low reduction potential, have been found to be electron carriers in a variety of biochemical reactions. The "plant-type" protein was first isolated from spinach chloroplasts, but is now known to be present in all photosynthetic organisms that utilize water as an electron donor and produce oxygen [1]; and the "two-iron" proteins are found in plants, bacteria and mammals [1]. The number of amino acid residues for these proteins varies between 97 and 112 [1]. The proteins are diamagnetic in the oxidized state at low temperatures and paramagnetic in the reduced state and exhibit EPR spectra below 140 K. characteristic of an effective $S = 1/2$ system.

In 1968, when much of our collaborative work on ferredoxins began, the proteins containing the [2Fe-2S] cluster were divided into two groups (by Beinert) based on their EPR spectra. Parsley ferredoxin, spinach ferredoxin, and azotobacter Fe-S Protein II are members

* Corresponding author. Fax: 1-734-763-3474.
E-mail address: wrdunham@umich.edu (W.R. Dunham).

0006-291X/$ - see front matter © 2003 Elsevier Inc. All rights reserved.
doi:10.1016/j.bbrc.2003.09.228

of the "plant-type ferredoxins." Beinert and others renamed these "the Type I ferredoxins" as it became clear that there was nothing especially plant-like with these proteins. Putidaredoxin, azotobacter Fe-S Protein I, adrenodoxin, and *C. pasteurianum* paramagnetic protein became then "the Type II ferredoxins" by default. However, the two groups are easily distinguished on the basis of their g values. Type I ferredoxins have rhombic EPR spectra with g values near 1.89, 1.96, and 2.05. Type II ferredoxins have nearly axial spectra with g values near 1.94, 1.94, and 2.02.

Materials

The reader is referred to Fritz et al. [2] for a discussion of the preparation of the ENDOR samples employed here.

ENDOR

Electron-nuclear double resonance (ENDOR) is a well-established technique initiated by Feher for studying paramagnetic sites in single crystals [3]. Hyde and co-workers extended this to the study of free radicals in solution [4,5] and later to powdered samples containing paramagnetic ions [6].

In ENDOR the intensity of a partially saturated EPR spectrum is affected by applying to the sample a variable frequency radiofrequency field, which can induce nuclear spin transitions. Let us consider the phenomenon of ENDOR for a single unpaired electron ($S = 1/2$) interacting with a single nucleus ($I = 1/2$). We will further assume an isotropic hyperfine (Fermi contact) interaction between these two particles. The Hamiltonian describing this system in an applied static magnetic field H is

$$\begin{aligned}\mathscr{H} &= -\mu_e \cdot H - \mu_n \cdot H + AI \cdot S \\ &= +g_e\beta S \cdot H - \mu_n\beta_n I \cdot H + AI \cdot S, \end{aligned} \quad (1)$$

where $\mu_e = -g_e\beta S$ is the magnetic moment of the electron; $\mu_n = g_n\beta_n I$, the magnetic moment of the nucleus; A, the hyperfine constant; I, the nuclear spin; S, the electron spin; g_e, the electron g factor; g_n, the nuclear g factor; β, the Bohr magneton; β_n, the nuclear magneton; and H, the applied magnetic field. In high field the energies are given by

$$E = +g_e\beta m_S H - g_n\beta_n m_I H + A m_S m_I. \quad (2)$$

Fig. 1A displays the energy levels as a function of applied magnetic field and Fig. 1B, the energy levels at high field, where each level is labeled at the side by the electron spin quantum number, m_S, and above by the nuclear quantum number, m_I. [For ^{57}Fe in these studies, $A \gg g_n\beta_n H$, and for protons at a distance from the center such as the protons in the cysteine, $A \ll g_n\beta_n H$.] The dotted lines in Fig. 1B denote the principal relaxation paths given an isotropic A (there are others). The relaxation rate at which direct nuclear transitions occur is denoted by $1/\tau_n$, the rate at which electron transitions occur by $1/\tau_1$, and the rate at which cross-relaxation occurs by $1/\tau_x$. Most generally, $\tau_1 \ll \tau_x \ll \tau_n$.

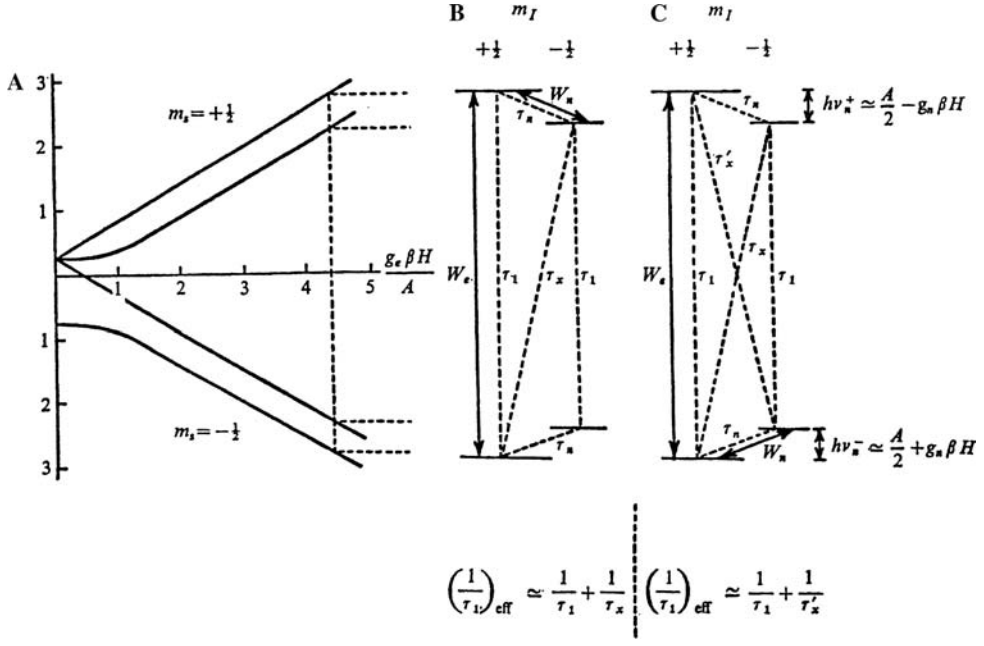

Fig. 1. (A) The energy level diagram as a function of H for an $S = 1/2$, $I = 1/2$ system with $I \cdot S$ coupling ($A \gg g_n\beta_n H$). (B) The energy levels and relaxation paths (dotted lines) at a fixed applied magnetic field with the $\Delta m_S = \pm 1$, $m_I = 1/2$ transition induced at a rate $W_e \gg 1/\tau_x$ and the $\Delta m_I = \pm 1$, $m_S = +1/2$ transition induced at a rate $W_n \gg 1/\tau_x$. (C) The same as (B) but with an anisotropic hyperfine coupling and the $\Delta m_I = \pm 1$, $m_S = -1/2$ transition induced at $W_n \gg 1/\tau'_x$.

In ENDOR, one induces the electronic transition at a rate, W_e, which is fast compared to $1/\tau_x$ and tends to equalize the populations in these two electronic states so that when one also induces the nuclear transition at a rate, W_n, fast compared to $1/\tau_x$ the population of the $m_S = +1/2,\ m_I = +1/2$ state is strongly affected. This results in a pronounced increase in the power absorbed in the electronic transition, which is easily detected.

In the case of anisotropic A, transitions between the $m_S = +1/2,\ m_I = +1/2$ and $m_S = -1/2,\ m_I = -1/2$ states are allowed and a new relaxation path is created with a characteristic relaxation time τ'_x as shown in Fig. 1C. The two nuclear transitions now result in ENDOR signals that will not be equal in general. With this in mind, a hypothetical ENDOR spectrum may be constructed using Eq. (2) to obtain the nuclear transition frequencies $h\nu_n^{\pm} = |g_n\beta H \pm A/2|$, which shows that two lines will be observed corresponding to the two values of m_S and they will be centered at frequencies given by the above equation. For ^{57}Fe here, $A/2 \gg g_n\beta_n H$, and for protons here, the reverse is true.

Anisotropic g and A tensors. In systems that have anisotropic g and A tensors, the iron ENDOR spectra would look like the pair predicted above for any given molecular orientation; however, for a frozen solution of protein molecules, all orientations are present and the spectra are complicated by the resulting superposition of spectra from a variety of orientations. Not all orientations contribute to the ENDOR spectra, because not all orientations are undergoing EPR. From the discussion in Fritz et al. [2], one sees that it is possible that by selecting the magnetic field, one may select molecules of various orientations to undergo EPR and hence ENDOR; thus it is possible to obtain the values of the components of the effective A tensor along the principal axes directions for the g tensor, and even decide how the A tensor principal axes are rotated with respect to the g tensor principal axes. A computer program is required to do this.

The synthesis of EPR spectra for amorphous samples has been discussed by several authors, but once again for simplicity, the reader is referred to Fritz et al. [2] for the history and a discussion of the synthesis of EPR spectra for samples with all orientations present as in our case of frozen amorphous solutions. For our purposes, it is sufficient to display in Fig. 2 the expected EPR spectrum for a frozen amorphous solution of a molecule with an anisotropic g tensor ($g_x < g_y < g_z$ as for Type I ferredoxins). Notice that $H_x = h\nu_0/g_x\beta$ is the magnetic field at which molecules having their g tensor x axes collinear with the applied field will absorb microwave power; i.e., undergo EPR. Similarly, $H_z = h\nu_0/g_z\beta$ is the magnetic field at which molecules having their z axes collinear with the applied field will absorb; since $H_z < H_y < H_x$ by assumption, $H_y = h\nu_0/g_y\beta$ is the magnetic field where not only molecules with their y axes aligned collinear with the field will absorb but also any molecule with the magnetic field lying anywhere in the plane formed by the y axis and a line in the x, z plane where the g value is equal to g_y. For this reason there is a much greater EPR intensity at H_y.

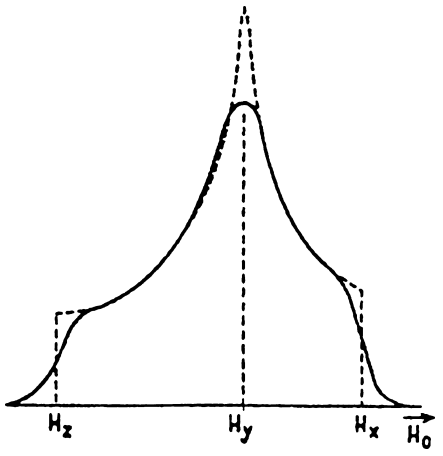

Fig. 2. A calculated integrated EPR absorption spectrum resulting from an amorphous sample with $H_z < H_y < H_x$, where $H_i = h\nu_0/g_i\beta$. The dotted lines represent dN/dH, the number of molecules with an absorption center located between H and $H + dH$, and the solid curve is the actual absorption curve resulting from a Gaussian absorption spectrum for each molecule. From Fritz et al. [2].

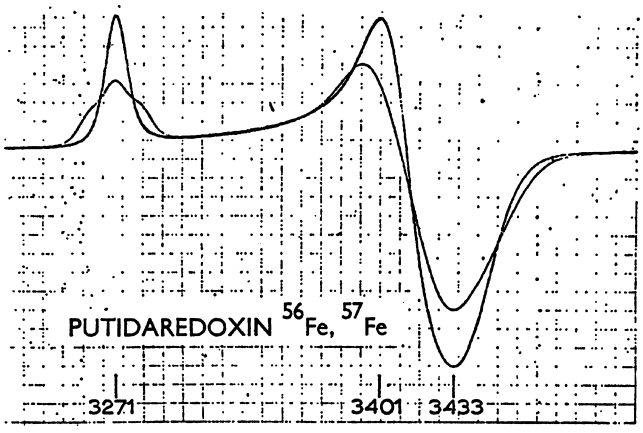

Fig. 3. The EPR derivative spectra from reduced putidaredoxin reconstituted with ^{56}Fe (narrow spectrum) and ^{57}Fe (broad spectrum). Attention is called to the 1:2:1 triplet splitting at H_z (3271 gauss) for the ^{57}Fe ($I = 1/2$) proteins. From Tsibris et al. [7].

Fig. 3 displays the derivative of the EPR spectrum (the magnetic field is modulated sinusoidally and the resulting EPR signal phase-detected) observed for putidaredoxin. Notice that for this protein, $g_x \cong g_y \cong g_\perp$; i.e., the g tensor is nearly axial (Type II ferredoxins).

Fig. 4 displays the ENDOR spectra observed for ^{56}Fe and ^{57}Fe substituted putidaredoxin when the applied radiofrequency radiation (to induce the nuclear transitions) is swept mechanically from 6 to 30 MHz. Fig. 4A shows the spectra obtained when the magnetic field is set so as to select those molecules whose z axes are aligned

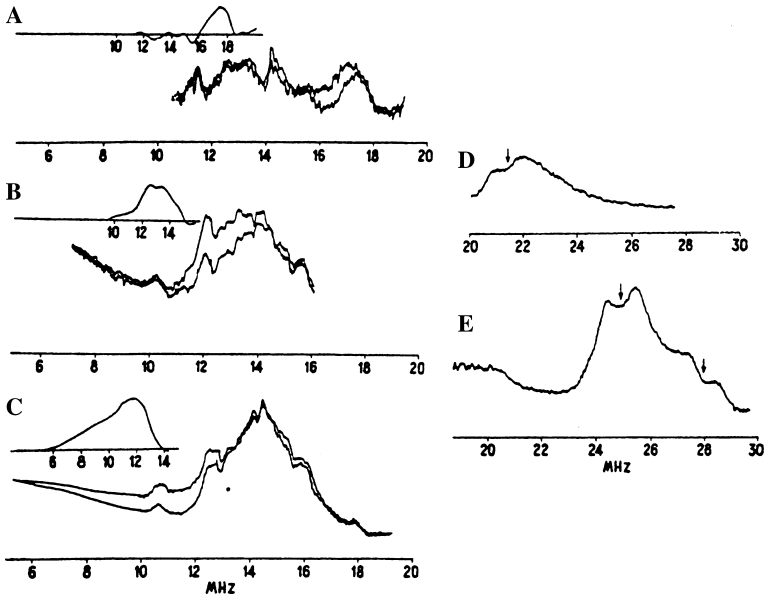

Fig. 4. The ENDOR spectra at 13 K and $\nu_0 = 9250$ MHz for reduced putidaredoxin in ^2H_2O reconstituted with ^{57}Fe (upper trace) or ^{56}Fe (lower trace) with the magnetic field set at (A and D) H_z, (B) $H_\perp$ - 31 G and (C and E) $H_\perp$. From Fritz et al. [2].

along the applied field. Note the difference spectrum centered around 17.5 MHz, which can be attributed to ^{57}Fe. (The underlying ENDOR is from protons whose nuclear magnetic resonance spectra are centered on 14 MHz.) Fig. 4D shows a continuation of the radio-frequency sweep above 20 MHz for the ^{57}Fe-enriched sample with the magnetic field set to select only those molecules whose z axes are along the applied field. The ^{56}Fe sample showed no ENDOR signals in this region. Thus there are two different iron ENDOR signals, one centered around 17.5 MHz and one pair centered about 21.5 MHz, presumably corresponding to two distinctly different iron sites in the active center of this protein, one with $A_z = 35$ MHz and one with $A_z = 43$ MHz. (The fact that these iron sites have A_z values within 20% of each other accounts for the apparent 1:2:1 triplet observed in the EPR spectrum of the ^{57}Fe sample at H_z. see Fig. 3.) Similarly, Fig. 4B shows the spectra obtained when the magnetic field is set at $H_\perp$ - 31 G to select molecules of orientations having the magnetic field intermediate between the z axis and the x-y plane; notice that the difference spectrum has shifted to lower frequencies. Likewise, Fig. 4C shows the ENDOR spectra obtained when the magnetic field is set at $H_\perp$ to select those molecules where the magnetic field is in the x-y plane. The difference spectrum has shifted to still lower frequencies and is broad. Similarly, Fig. 4E displays the ENDOR signals observed in the 20 to 28 MHz range for the ^{57}Fe sample with the magnetic field set in the x-y planes of the molecules. The ^{56}Fe sample shows no ENDOR signals in this region. Again, there are two distinctly different ^{57}Fe sites in this protein, one with its ENDOR signals centered around 10.5 MHz and the other with two pairs of ENDOR signals centered around 25 and 28 MHz, respectively, presumably corresponding to two different principal axis values in the x-y plane, namely, $A_y/2$ and $A_x,/2$, respectively. From the Mössbauer data of Dunham et al. [8] it was shown that one of the iron atoms was high-spin ferrous and the other consistent with high-spin ferric, which are consistent with the model proposed by Gibson et al. [9] of a high-spin ferric spin-coupled antiferromagnetically to a high-spin ferrous atom to form a net spin of 1/2 for the complex. This model of the antiferromagnetic coupling predicts the magnetic susceptibility with only one adjustable parameter, J, the exchange coupling $(-2JS_1 \cdot S_2)$. This may be obtained from the temperature dependence of the susceptibility as was done by Moss et al. [10], Petering and Palmer [11], and Palmer et al. [12]. Palmer et al. [12] obtained good fits to the temperature dependence assuming $J = 80\,\mathrm{cm}^{-1}$ in the ground state as well as an excited state at $400\,\mathrm{cm}^{-1}$ with a $J = -175\,\mathrm{cm}^{-1}$.

Using the results of Palmer et al. [14], Dunham et al. [13] calculated the expected temperature dependence of the expectation value of S_z at the ferric and ferrous atoms, respectively, assuming several different values of J consistent with the susceptibility data.

It is appropriate at this point to summarize the results of all of the experiments including the optical [14] and Mössbauer [8] studies, both of which indicate a distorted tetrahedral environment for each iron atom. To satisfy the latter requirement, one can assume that each iron atom is bound to four sulfur atoms, two from the acid-labile sulfur atoms which are assumed to bridge the iron atoms and two from cysteine sulfur atoms. If the latter assumption is true, then the model is that shown in Fig. 5. Notice that the spin density on the iron atoms

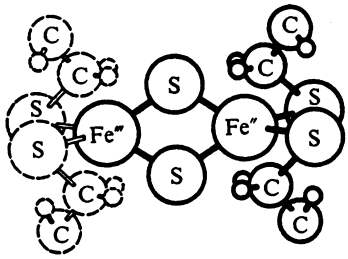

Fig. 5. Schematic structure of the iron–sulphur complex in the two-iron ferredoxins. From Dunham et al [13].

should overlap the α-CH and β-CH_2 protons of each cysteine ligand. Using the temperature dependences of the expectation values of S_z at each iron atom, Dunham et al. [13] predicted the temperature dependence of the paramagnetic shifts of the various protons as observed at room temperatures by Poe et al. [15] and Salmeen and Palmer [16]. The results are shown in Fig. 6. The agreement offers strong support for the model shown in Fig. 5. Subsequent X-ray data on a two-iron model compound, the $[FeS(SCH_2)_2C_6H_4]_2^{2-}$ anion, by Mayerle et al. [18], showed a structure similar to the model in Fig. 5 with similar optical, Mössbauer spectra, magnetic susceptibility, redox potentials, and PMR spectra as those of the two-iron ferredoxins. Finally, X-ray crystallography [19] was done on several proteins with two-iron ferredoxin type centers to confirm the structure.

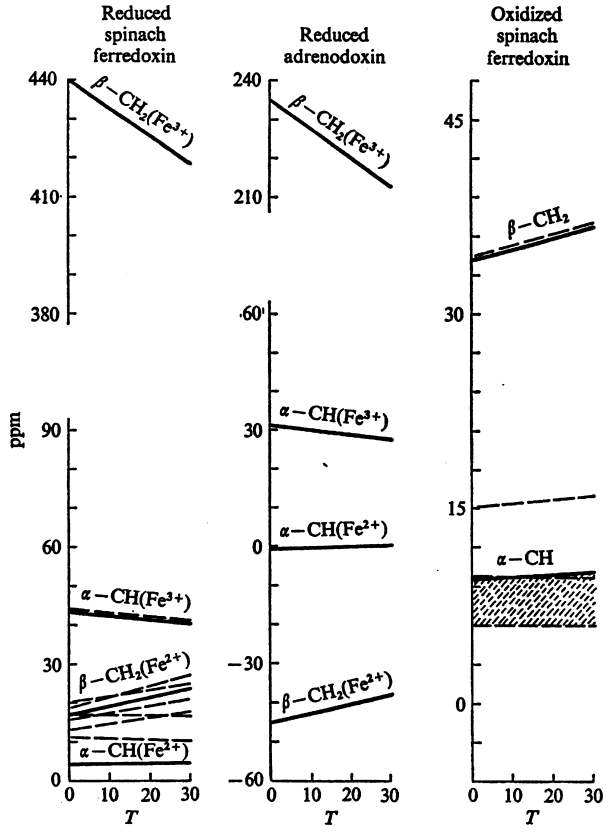

Fig. 6. PMR energies vs temperature for structure in Fig. 5. Ordinate given in parts per million; positive values of ppm refer to resonances downfield relative to 2,2-dimethylsilapentane 5-sulphonic acid. Predicted line positions are shown in solid lines; dashed lines and shaded areas indicate the position of measured lines (Poe et al. [15]; Salmeen and Palmer [16]). This is changed from that shown in Dunham et al. [13] to take account of Salmeen's data wherein the β-CH_2 protons are shown to be at 37 ppm in the oxidized protein and the line at 43 ppm in the reduced protein is interpreted as the α-CH protons attached to the Fe^{3+}. The correspondence between the predicted and observed temperature dependences is strong support for this model. From Sands and Dunham [17].

g-Strain

G values describe the relationship between the applied magnetic field $\vec{\mathbf{H}}$ and the angular momentum $\vec{\mathbf{S}}$ of the paramagnetic site. Because that relationship depends on the orientation of the protein in the applied magnetic field, the interaction of the two vectors is described using a tensor: $E = \vec{\mathbf{H}} \cdot \beta\tilde{\mathbf{G}} \cdot \vec{\mathbf{S}}$, where E is the energy of the interaction, β is the Bohr magneton, and $\tilde{\mathbf{G}}$ is the g tensor. A tensor describes a vectorial relationship that differs with orientation; for example, the relationship between the force on an object (stress) and the deformation of the object (strain) is described by a tensor. Obviously, this depends on the object. However, with a proper definition, a single tensor can completely describe the relationship between the two vectors. For the ferredoxins, this property of tensors is insufficient to describe the magnetic moment $\beta\tilde{\mathbf{G}} \cdot \vec{\mathbf{S}}$ of the active site of these proteins, as we will see below.

The **G** tensor often characterizes the extent of an EPR signal, with the first maximum, the crossover and the final minimum of an EPR spectrum located near the three principal g values for the spin system. On the other hand, the linewidth of an EPR signal is also a function of direction: differing for the three principal directions and visible as the width of the spectral resonance at the three turning points often as a full width at half maximum (see Fig. 2). This linewidth has many contributors. The most fundamental (but not the largest for ferredoxins) contribution is that given by the transverse relaxation time in the Bloch equations. This number was known to us (because it is one-half the experimental linewidth from the ENDOR experiments on these proteins) as ~125 kHz, which translates to ~0.05 G. The ENDOR experiments also identified several contributions to the linewidths from several nuclei (^1H, ^{13}N, ^{14}N, ^{57}Fe) of a few MHz (tenths of Gauss). However, the EPR spectra under investigation had linewidths of several Gauss. Therefore, we were somewhat mystified about the origin of this linewidth. Furthermore, when we studied the EPR spectra at several microwave frequencies (and applied magnetic field as a result), we found that the linewidth scaled approximately with the frequency. Because none of the contributions considered above would be frequency dependent, we were forced to

conclude that main linewidth contribution in the ferredoxin EPR spectra was field dependent. Thus, the linewidth could be considered to originate from the "*g*-tensor distribution." We termed this phenomenon "*g*-strain."

Simultaneously with this experimental work, the computer synthesis of EPR spectra also took several steps forward. Roland Aasa [20] had pointed out that although these spectra were generated as "H-field-swept spectra," the individual resonances forming a powder spectrum were properly normalized in frequency space. Therefore, the resonances generated in this way should be renormalized by dividing each by a factor, *g*, the spectroscopic splitting factor. Bill Blumberg [21] added that this was only necessary if spectra were generated in this simple way and that many computer programs avoided the problem in other ways. In our own laboratory, Lou Strong [22] derived a lineshape in frequency-space and projected this lineshape into field-space with a proper functional form (asymmetric) and a proper evaluation of the Jacobian, thus re-deriving the Aasa correction. In the Netherlands, Fred Hagen [23] wrote a computer program that came the closest to synthesizing the ferredoxin using an expression that emphasized an absolute value in the linewidth algorithm.

Upon completing his doctoral work, Fred Hagen came to our laboratory to work with us. Naturally, he retained his interest in the *g*-strain problem. His arrival coincided with the thesis work of David Hearshen, a predoctoral student in our laboratory, who had applied multivariate analysis techniques to the same problem. Working together, they were able to show that Fred Hagen's algorithm was a special case of the theory that resulted from Dave's work.

The thesis of Dave Hearshen posits that the *g* value from an EPR spectrum arises from a distribution of spin systems with a mean *g* value and a linewidth that derives from a random vector quantity, independent of the *g* value. A ton of mathematics results from properly treating a quantity as a random vector, including Euler rotations, correlation coefficients and principal *g* strain parameters. The difficulty in fitting the ferredoxin EPR spectra centers to the asymmetric shape at the center of these spectra. This asymmetry results from very narrow linewidths caused by full negative correlation among the linewidth parameters and the fact that the coordinate system of these linewidth parameters is not aligned with that of the *g* value means. The reader is referred to Refs. [24–26] for a detailed discussion of the mathematics and the parameters for particular proteins.

To be sure, this mathematics is complicated and not at all common to most biochemistry laboratories. However, once the decision is made that the concept of a single *g* tensor is inappropriate for these EPR spectra, it should not be expected that its alternative is mathematically simple. In fact, abandoning the concept of a *g* tensor is probably more important than the multivariate analysis that took its place. The structural importance of this conclusion is that a protein structure cannot be considered unique, but that it contains a distribution of structures—a distribution that gives rise to *g*-strain. Amazingly, this distribution is present even in single crystal, as EPR spectra of ferredoxins in collaboration with Martha Ludwig [27] have shown. As Hans Frauenfelder has stated [28], the apparent picture is one where the structure is less specified the further one travels from the center of the protein. This brings us back to the University of Illinois, home of Frauenfelder and Gunsalus.

Acknowledgments

Much of the work described in the preceding pages as coming from our own laboratories was supported by National Institute of Health Research Grant GM 12176 and was done in collaboration with a large number of colleagues, including Dr. H. Crespi, Argonne National laboratories; Dr. A. Bearden, University of California, Berkeley; Drs. H. Beinert and W. Orme-Johnson, University of Wisconsin; Drs. I.C. Gunsalus and J. Tsibris, University of Illinois; Dr. H.J. Grande, Wageningen University, Dr. I. Salmeen, Ford Scientific Laboratories; and Dr. G. Palmer, J. Fritz, D. Petering, and R. Anderson, University of Michigan.

References

[1] The reader is referred to the introduction in Fritz et al. [2] for references to the early biochemical studies.
[2] J. Fritz, R.E. Anderson, J.A. Fee, G. Palmer, R.H. Sands, J.C.M. Tsibris, I.C. Gunsalus, W.H. Orme-Johnson, H. Beinert, The iron electron nuclear double resonance (ENDOR) of two-iron ferredoxins from spinach, parsley, pig adrenal cortex and *Pseudomonas putida*, Biochim. Biophys. Acta 253 (1971) 110–133.
[3] G. Feher, Electron spin resonance experiments on donors in silicon. I. Electronic structure of donors by the electron nuclear double resonance technique, Phys. Rev. 114 (1959) 1219–1244.
[4] J.S. Hyde, A.H. Maki, ENDOR of a free radical in solution, J. Chem. Phys. 40 (1964) 3117–3118.
[5] J.S. Hyde, ENDOR of free radicals in solution, J. Chem. Phys. 43 (1965) 1806–1818.
[6] G.H. Rist, J.S. Hyde, Ligand ENDOR of metal complexes in powders, J. Chem. Phys. 52 (1970) 4633–4643, and earlier publications referenced therein.
[7] J.C.M. Tsibris, R.C. Tsai, I.C. Gunsalus, W.H. Orme-Johnson, R.E. Hansen, H. Beinert, The number of iron atoms in the paramagnetic center ($g = 1.94$) of reduced putidaredoxin, a non heme iron protein, Proc. Natl. Acad. Sci. USA 59 (1968) 959–965.
[8] W.R. Dunham, A. Bearden, I. Salmeen, G. Palmer, R.H. Sands, W.H. Orme-Johnson, H. Beinert, The 2-iron ferredoxins in spinach, parsley, pig adrenal cortex, *Azotobachter vinelandii* and *Clostridium pasteurianum*: studies by magnetic field Mössbauer spectroscopy, Biochim. Biophys. Acta 253 (1971) 134–152.
[9] J.F. Gibson, D.O. Hall, J.H.M. Thornley, F.R. Whatley, The iron complex in spinach ferredoxin, Proc. Natl. Acad. Sci. USA 56 (1966) 987–990.
[10] T.H. Moss, D. Petering, G. Palmer, The magnetic susceptibility of oxidized and reduced ferredoxin from spinach and parsley and the

high potential protein from chromatium, J. Biol. Chem. 244 (1969) 2275–2277.
[11] D. Petering, G. Palmer, Properties of spinach ferredoxin in anaerobic urea solutions: a comparison with the native protein, Arch. Biochem. 141 (1970) 456–464.
[12] G. Palmer, W.R. Dunham, J.A. Fee, R.H. Sands, T. Iizuka, I. Yonetani, The magnetic susceptibility of spinach ferredoxin from 77–250 °K: a measurement of the antiferromagnetic coupling between the two iron atoms, Biochim. Biophys. Acta 245 (1971) 201–207.
[13] W.R. Dunham, G. Palmer, R.H. Sands, A.J. Bearden, On the structure of the iron–sulphur complex in the 2-iron ferredoxins, Biochim. Biophys. Acta 253 (1971) 373–384.
[14] W. Eaton, G. Palmer, J.A. Fee, T. Kimura, W. Lovenberg, Tetrahedral iron in the active center of plant ferredoxin and beef adrenodoxin, Proc. Natl. Acad. Sci. USA 68 (1971) 3015–3020.
[15] M. Poe, W.D. Phillips, J.D. Glickson, A. San Pietro, Proton magnetic resonance studies of the ferredoxins from spinach and parsley, Proc. Natl. Acad. Sci. USA 68 (1971) 68–74.
[16] I.T. Salmeen, G. Palmer, Contact-shifted NMR of spinach ferredoxin additional resonances and partial assignments, Arch. Biochem. Biophys. 150 (1972) 767–773.
[17] R.H. Sands, W.R. Dunham, Spectroscopic studies on two-iron ferredoxins, Q. Rev. Biophys. 7 (1975) 443–504.
[18] J.J. Mayerle, R.B. Frankel, R.H. Holm, J.A. Ibers, W. Phillips, J.F. Weiher, Synthetic analogss of the active sites of the iron-sulfur proteins: structure and properties of Bis [*o*-xyldithiolate-u_2-sulfidoferrate(III)]: an analog of the 2Fe-2S proteins, Proc. Natl. Acad. Sci. USA 70 (1973) 2429–2433.
[19] See, for example, Fig. 12 in T. Tsukahara, K. Fukayama, M. Nakamura, Y. Katsube, N. Tanake, M. Kakudo, K. Wado, T. Hase, H. Matsubara, X-ray analysis of a [2Fe-2S] ferredoxin from *Spirulina platensis*, main chain fold and location of side chains at 2.5 Å resolution, J. Biochem. 90 (1981) 1763–1773.
[20] R. Aasa, T. Vanngard, EPR signal intensity and powder shapes: a reexamination, J. Magn. Reson. 19 (1975) 308–315.
[21] W. Blumberg, personal communication to W.R.D.
[22] L.H. Strong, Biophysical studies on selected iron-sulfur proteins, Ph.D. thesis (physics), University of Michigan (1976).
[23] W.R. Hagen, S.P.J. Albracht, Analysis of strain-induced EPR-line shapes and anisotropic spin lattice relaxation in a 2Fe-2S ferredoxin, Biochim. Biophys. Acta 702 (1982) 61–71.
[24] W.R. Hagen, D.O. Hearshen, R.H. Sands, W.R. Dunham, A statistical theory for powder EPR in distributed systems, J. Magn. Reson. 61 (1985) 220–232.
[25] W.R. Hagen, D.O. Hearshen, L.J. Harding, W.R. Dunham, Quantitative numerical analysis of g strain in the EPR of distributed systems and its importance for multicenter metalloproteins, J. Magn. Reson. 61 (1985) 233–244.
[26] D.O. Hearshen, W.R. Hagen, R.H. Sands, H.J. Grande, H.L. Crespi, I.C. Gunsalus, W.R. Dunham, An analysis of g strain in the EPR of two [2Fe-2S] ferredoxins: evidence for a protein rigidity model, J. Magn. Reson. 69 (1986) 440–459.
[27] This work is unpublished in collaboration with M.L. Ludwig, D. Gatti, D.P. Ballou, on single crystals of phthalate dioxygenase reductase.
[28] H. Frauenfelder, G.A. Petsko, D. Tsernoglou, Temperature-dependent X-ray diffraction as a probe of structural dynamics, Nature 280 (1979) 558–563.